

Hydrogen diffusion coefficient, hydrogen solution coefficient and hydrogen permeability of Nb-TiNi eutectic alloy

Weiliang Wang^{1, a}, Kazuhiro Ishikawa^{2, b} and Kiyoshi Aoki^{3, c}

^{1, 2, 3} Department of Materials Science and Engineering, Kitami Institute of Technology, Kitami
 090-8507, Japan

^c aokiky@mail.kitami-it.ac.jp

Keywords: Hydrogen permeable membrane; Hydrogen diffusion; hydrogen solution; Nb-TiNi alloy

Abstract: In general, hydrogen permeability Φ of the alloy membrane is expressed as the product of the hydrogen diffusion coefficient D and the hydrogen solution coefficient K . Therefore, to improve the hydrogen permeability efficiently, the values of K and D should be separately considered. In the present study, hydrogen absorption and permeation behaviors of the Nb₁₉Ti₄₀Ni₄₁ alloy consisting of the eutectic phase are investigated by measuring pressure-composition-isotherm (PCI) and by the hydrogen flow method and compared with those of palladium. The hydrogen absorption in the Nb₁₉Ti₄₀Ni₄₁ alloy does not obey the Sieverts' law in the pressure region of 0-1.0MPa at 523K, but it shows linear relationship between the difference in the square root of hydrogen pressure and hydrogen content between 0.1 and 0.4MPa. Although the value of D for the Nb₁₉Ti₄₀Ni₄₁ alloy is considerably lower than that of palladium, its high K value enhances the hydrogen permeability Φ . It is suggested that the enhancement of D by microstructural control for Nb₁₉Ti₄₀Ni₄₁ alloy is effective for improvement of Φ .

1. Introduction

Palladium-silver alloys have been used as hydrogen permeation membranes for separation and purification of hydrogen gas [1, 2]. However palladium is expensive and a rare metal, so that it is urgent to develop new, low cost and high performance non-palladium-based hydrogen permeation alloys. Recently, the Nb-TiNi alloys which consist of the primary bcc-(Nb, Ti) and the eutectic {bcc- (Nb, Ti) + B2- TiNi} phases have attracted wide attention because of their high Φ values and excellent resistance to hydrogen embrittlement [3, 4]. It has been explained that the hydrogen permeation is mainly determined by the primary phase, while the suppression of hydrogen embrittlement is mainly controlled by the eutectic one [5]. However it is not experimentally elucidated that the relationship of Φ , D and K in these alloys.

In general, the diffusion flux (J) of hydrogen in the metal membrane is given by Fick's first law as follows.

$$J = -D \times dC/dx = D \times (C_u - C_d)/L \quad (1)$$

Where D represents the diffusion coefficient of hydrogen in solids, C_u and C_d are the hydrogen content in the solid just beneath the surfaces in the upstream and the downstream sides, respectively. L is the thickness. The hydrogen concentration gradient is the driving force of the hydrogen diffusion. Hydrogen permeation thorough the metal membrane is schematically shown in Fig.1.

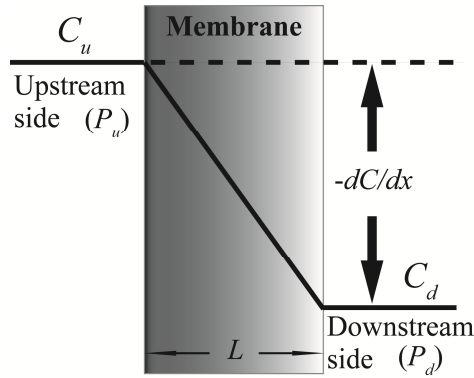


Figure 1 The schematic illustration of hydrogen permeation.

When the hydrogen concentration is low, the relation between the equilibrium hydrogen content C and hydrogen partial pressure are given by Sieverts' law as follows:

$$C = K \times P^{0.5} \quad (2)$$

Then, the Fick's first law can be rewritten as follows,

$$J = DK(P_u^{0.5} - P_d^{0.5})/L \quad (3)$$

In practice, the membrane is used in the high hydrogen concentration region where the Sieverts' law is inapplicable. In such a case, if the hydrogen content is expressed as follows,

$$C = K \times P^{0.5} + \alpha \quad (4)$$

Then, the hydrogen flux is written as follows.

$$J = DK(\Delta P^{0.5})/L = \Phi(\Delta P^{0.5})/L \quad (5)$$

Here, D and K are the hydrogen diffusion coefficient and the hydrogen solution coefficient, respectively. The product of them is hydrogen permeability (Φ). $\Delta P^{0.5}$ and L are the difference of square root of the hydrogen pressure at both sides of the membrane and its thickness, respectively. If values of Φ and K are experimentally measured, then the value of D can be calculated by using Eq. (5). In the present study, K and Φ of the $\text{Nb}_{19}\text{Ti}_{40}\text{Ni}_{41}$ alloy consisting of the eutectic {bcc-(Nb, Ti) + B2-TiNi} phase [6] are determined by measuring the pressure-composition-isotherm (PCI) and by the gas flow method, respectively. Then, the value of D is evaluated by using Eq. (5). Furthermore, the values of D and K of the $\text{Nb}_{19}\text{Ti}_{40}\text{Ni}_{41}$ alloy are compared with those of palladium, and the controlling factor for hydrogen permeation of this alloy is discussed.

2. Experimental

Palladium and $\text{Nb}_{19}\text{Ti}_{40}\text{Ni}_{41}$ alloys (mol%) were used in the present study. Palladium (99.98 mass%) was purchased from Tanaka Co., Japan. The $\text{Nb}_{19}\text{Ti}_{40}\text{Ni}_{41}$ alloy was prepared by arc melting in a purified argon atmosphere using Nb (99.9 mass%), Ti (99.5 mass%) and Ni (99.9 mass%). The samples of 12mm in diameter and 0.75 mm in thickness were cut from this alloy ingot by a spark erosion wire-cutting machine for the hydrogen permeation experiments. The rectangular parallelepiped samples of 12 mm \times 12mm \times 0.75 mm were cut for hydrogen absorption experiments. Microstructural and structural examinations were carried out with a scanning electron microscope (SEM, JSM 5300) and an X-ray diffractometer (XRD, PANalytical X'Pert PRO),

respectively. After both sides of these disks were polished using buff with $0.5\mu\text{m}$ Al_2O_3 particles, palladium was coated with 190 nm thicknesses using a DC sputtering machine to avoid oxidation and to enhance the dissociation of hydrogen molecule on the disks. After the alloy disk was sealed by gaskets, both sides of the sample were evacuated using a diffusion pump below 3×10^{-3} Pa, then heated to 673K and kept for 1.8 ks. Pure hydrogen gas (99.99999%) of 0.2-0.4 MPa and 0.1 MPa was introduced in the upstream side and in the downstream side, respectively. Hydrogen flux J passing through the disk was measured by a hydrogen flow meter (KOFLOC Model-3300), and the value of Φ was determined from the slope of the relation between $J \times L$ vs. $\Delta P^{0.5}$ plot. PCI was measured using a Sieverts-type apparatus. The amount of absorbed hydrogen was calculated from the change of the pressure and the inner volume of the chamber. The temperature of the sample was controlled to an accuracy of $\pm 1\text{K}$ during the measurement. Absorption experiments were carried out at 523K, and at pressures ranging from 0.01 to 1MPa.

3. Results and Discussion

3.1 Microstructure and crystal structure of the $\text{Nb}_{19}\text{Ti}_{40}\text{Ni}_{41}$ alloy

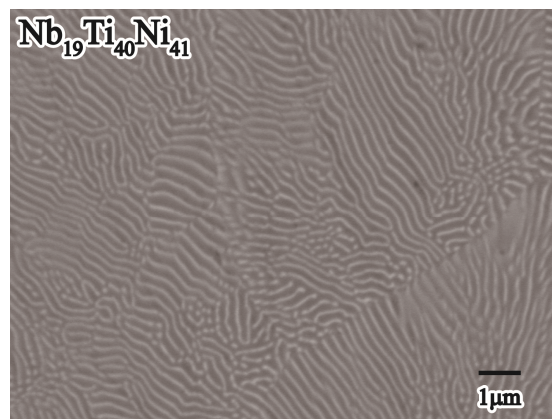


Figure 2 An SEM micrograph of the as-cast $\text{Nb}_{19}\text{Ti}_{40}\text{Ni}_{41}$ alloy.

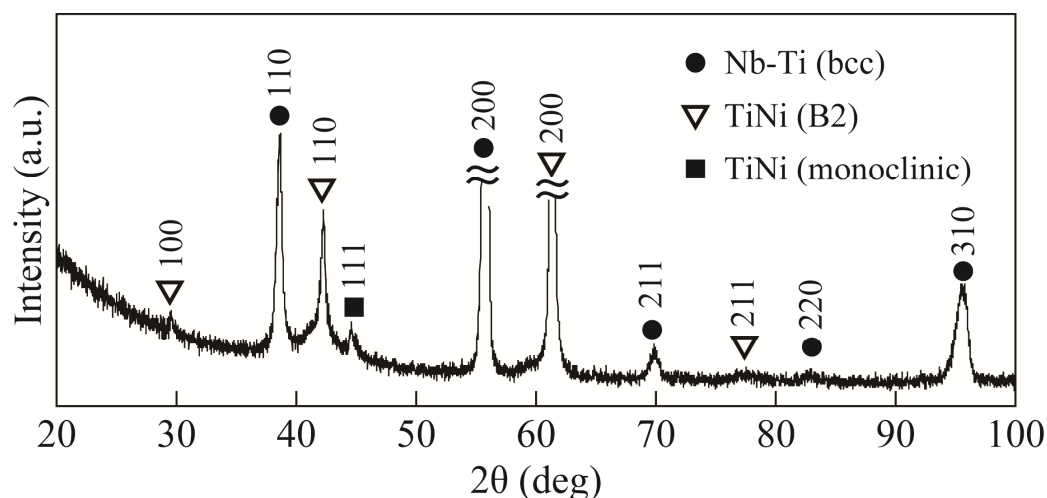


Figure 3 An X-ray diffraction pattern of the as-cast $\text{Nb}_{19}\text{Ti}_{40}\text{Ni}_{41}$ alloy.

Fig.2 and Fig.3 show an SEM photograph and an XRD pattern of the $\text{Nb}_{19}\text{Ti}_{40}\text{Ni}_{41}$ alloy, respectively. This alloy consists of the eutectic $\{\text{bcc- (Nb, Ti)} + \text{B2- TiNi}\}$ phase with fine lamellar microstructures in good agreement with the previous works [5, 6].

3.2 Hydrogen solution coefficient K and hydrogen content C of the $\text{Nb}_{19}\text{Ti}_{40}\text{Ni}_{41}$ alloy and palladium

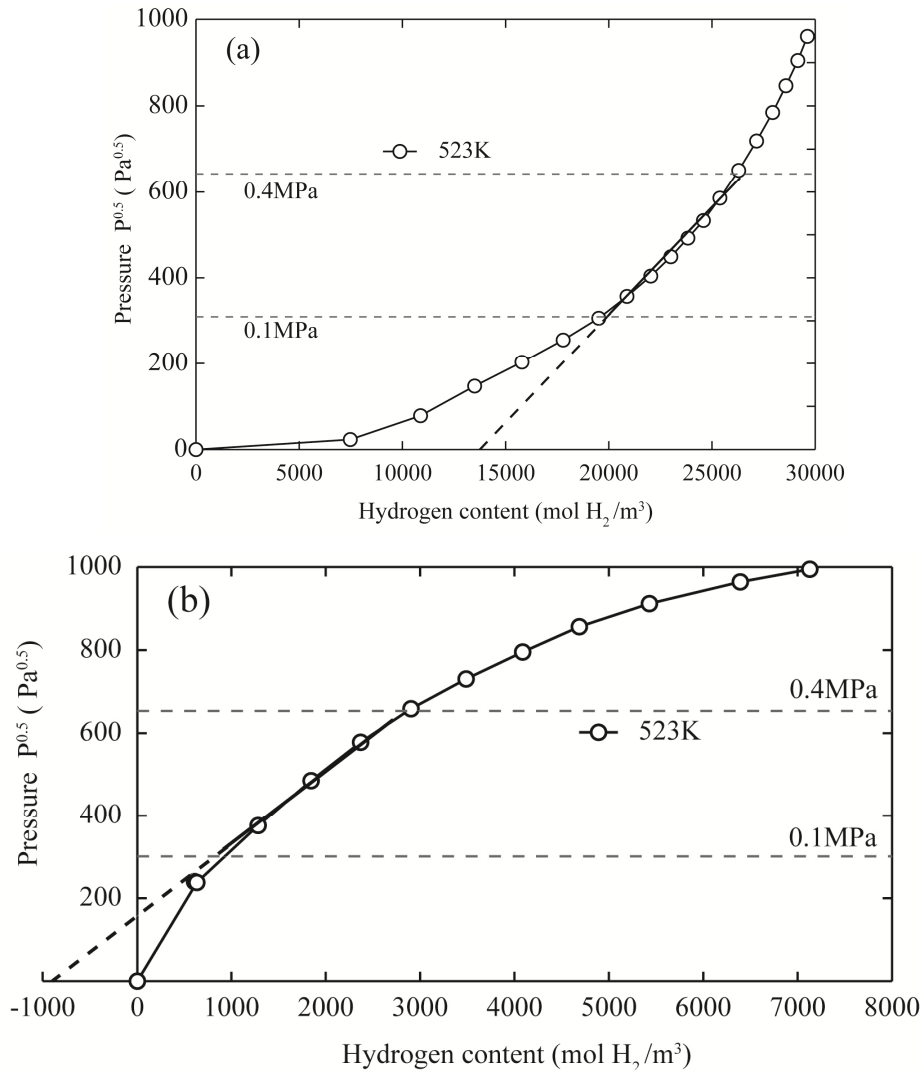


Fig. 4 (a) and (b) Hydrogen- pressure-composition isotherm (PCI) of the $\text{Nb}_{19}\text{Ti}_{40}\text{Ni}_{41}$ alloy (a) and palladium (b) at 523K.

Fig. 4 (a) and (b) show PCI for the $\text{Nb}_{19}\text{Ti}_{40}\text{Ni}_{41}$ alloy and palladium at 523K, respectively. In these Figures, the square root of the hydrogen pressure is plotted against the hydrogen content ($\text{mol H}_2/\text{m}^3$). The isotherms do not pass through the origin, which indicates that the Sieverts' law is not hold at the pressure region of 0- 1.0 MPa at 523K. However, PCI between 0.1 and 0.4MPa at 523K is roughly on the straight line. Then the relationship of the hydrogen content and the square root of hydrogen pressures can be expressed as $C = Kp^{0.5} + \alpha$. Here, C and K are the hydrogen content and the hydrogen solution coefficient, respectively. The values of K for the $\text{Nb}_{19}\text{Ti}_{40}\text{Ni}_{41}$ alloy and palladium are calculated from the gradient of these $PCIs$.

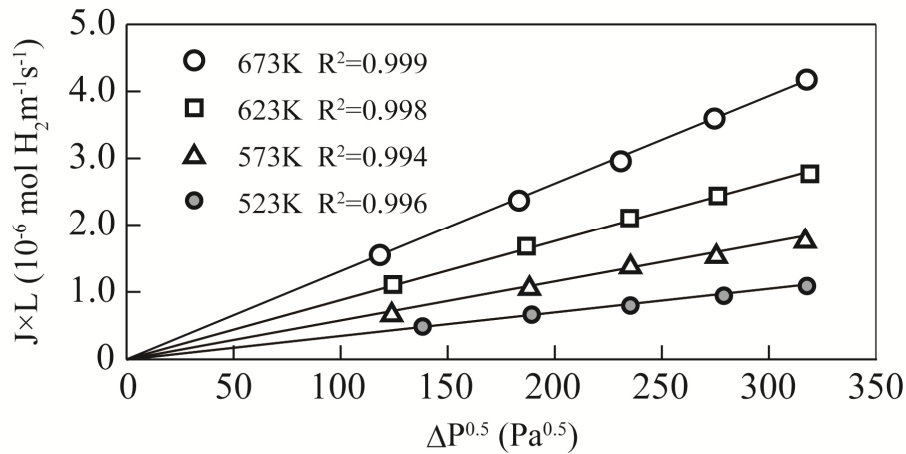


Figure 5 Typical plot of $(J \times L)$ vs. $\Delta P^{0.5}$ for $\text{Nb}_{19}\text{Ti}_{40}\text{Ni}_{41}$ alloy between 673K and 523K.

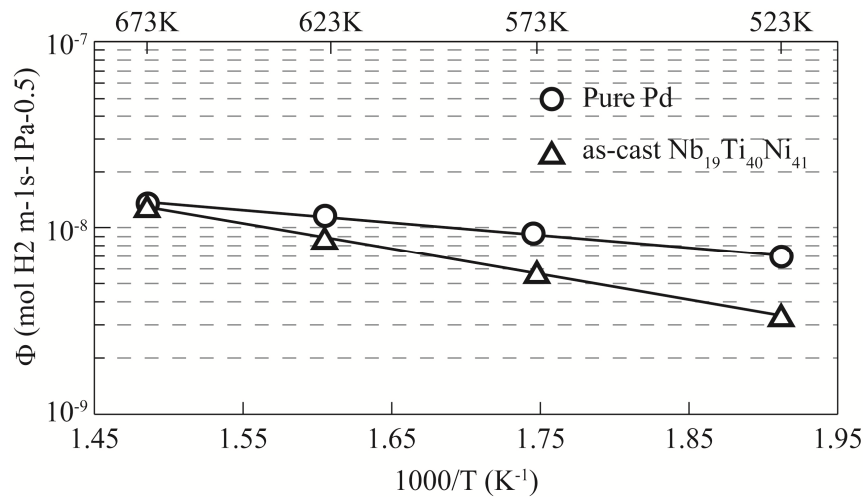


Figure 6 Temperature dependence of hydrogen permeability Φ for the $\text{Nb}_{19}\text{Ti}_{40}\text{Ni}_{41}$ alloy and palladium.

The hydrogen flux J is related to hydrogen permeability Φ as shown in Eq. (5). The $J \times L$ values are plotted against $\Delta P^{0.5}$ as shown in Fig. 5. The experimental data are on the straight lines passing through the origin. The gradient of these lines correspond to Φ at each temperature.

Figure 6 shows an Arrhenius plot of the hydrogen permeability Φ for the $\text{Nb}_{19}\text{Ti}_{40}\text{Ni}_{41}$ alloy and palladium. The value of Φ increases with increasing temperature, and the Φ value of the $\text{Nb}_{19}\text{Ti}_{40}\text{Ni}_{41}$ alloy is lower than that of palladium from 523K to 673K.

3.3 Hydrogen permeability Φ , hydrogen solution coefficient K and hydrogen diffusion coefficient D of the $\text{Nb}_{19}\text{Ti}_{40}\text{Ni}_{41}$ alloy and palladium

The values of Φ , K and D for the $\text{Nb}_{19}\text{Ti}_{40}\text{Ni}_{41}$ alloy and palladium at 523 K are listed in Table 1. The value of D for palladium is almost the same as that of Baykara [7]. The value of Φ for the $\text{Nb}_{19}\text{Ti}_{40}\text{Ni}_{41}$ alloy is 1/2 of palladium. The value of K for the $\text{Nb}_{19}\text{Ti}_{40}\text{Ni}_{41}$ alloy is 3 times higher than that of palladium. The value of D for the $\text{Nb}_{19}\text{Ti}_{40}\text{Ni}_{41}$ alloy is only 1/6 of that of palladium. The lower value of D for the $\text{Nb}_{19}\text{Ti}_{40}\text{Ni}_{41}$ alloy may result from the duplex phase schematically

shown in Fig.7. This suggests that the enhancement of D by the microstructural control is effective for improvement of hydrogen permeability Φ for the $\text{Nb}_{19}\text{Ti}_{40}\text{Ni}_{41}$ alloy.

Table 1 Hydrogen permeability Φ , hydrogen solution coefficient K and the hydrogen diffusion coefficient D for the $\text{Nb}_{19}\text{Ti}_{40}\text{Ni}_{41}$ alloy and palladium.

	523K		
	$\text{Nb}_{19}\text{Ti}_{40}\text{Ni}_{41}$	palladium	alloy/Pd
$\Phi [\text{molH}_2\text{m}^{-1}\text{s}^{-1}\text{Pa}^{-0.5}]$	3.4×10^{-9}	7.0×10^{-9}	1/2
$K [\text{molH}_2\text{m}^{-3}\text{Pa}^{-0.5}]$	17	6	3
$D [\text{m}^2\text{s}^{-1}]$	2.0×10^{-10}	1.2×10^{-9}	1/6

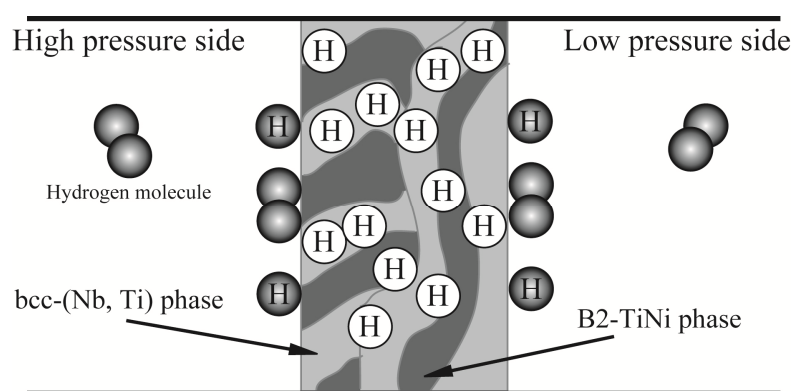


Figure 7 The lower D for the $\text{Nb}_{19}\text{Ti}_{40}\text{Ni}_{41}$ alloy due to the duplex phases.

4. Summary and Conclusion

The hydrogen concentration is approximated as $C = KP^{0.5} + \alpha$ between 0.1 and 0.4MPa at 523K for the $\text{Nb}_{19}\text{Ti}_{40}\text{Ni}_{41}$ alloy. The value of hydrogen diffusion D for $\text{Nb}_{19}\text{Ti}_{40}\text{Ni}_{41}$ alloy is lower than that of palladium. The bcc-(Nb, Ti) phase which exhibits high hydrogen permeability and the B2-TiNi phase which is excellent resistance to hydrogen embrittlement but low hydrogen permeability are mixed alternately as lamellar microstructures. It is suggested that the enhancement of D by the microstructural control is effective for improvement of hydrogen permeability Φ for the $\text{Nb}_{19}\text{Ti}_{40}\text{Ni}_{41}$ alloy.

References

- [1] E. Kikuchi: Catalysis Today, Vol. 56 (2000), p. 97
- [2] S. Uemiya, T. Matsuda and E. Kikuchi: J. Membr. Sci., Vol. 56 (1991), p. 315
- [3] K. Hashi, K. Ishikawa, T. Matsuda and K. Aoki: J. Alloy Compd., Vol. 268 (2004), p.215
- [4] K. Hashi, K. Ishikawa, T. Matsuda and K. Aoki: Mater. Trans., Vol. 46 (2005), p. 1026
- [5] W. Luo, K. Ishikawa and K. Aoki: Mater. Trans., Vol. 46 (2005), p. 2253
- [6] K. Kishida, Y. Yamaguchi, K. Tanaka, H. Inui, S. Tokui, K. Ishikawa and K. Aoki: Intermetallics, Vol. 16 (2008), p. 88
- [7] S. Z. Baykara: Int. J. Hydrogen Energy, Vol. 29 (2004), p. 1631